



Plate-shaped non-contact ultrasonic transporter using flexural vibration



Takahiko Ishii^{a,*}, Yosuke Mizuno^a, Daisuke Koyama^{a,b,c}, Kentaro Nakamura^a, Kana Harada^d, Yukiyoshi Uchida^d

^a Precision and Intelligence Laboratory, Tokyo Institute of Technology, 4259 Nagatsuta-cho, Midori-ku, Yokohama 226-8503, Japan

^b Faculty of Science and Engineering, Doshisha University, 1-3 Tataramiyakodani, Kyotanabe, Kyoto 610-0321, Japan

^c Wave Electronics Research Center, Doshisha University, 1-3 Tataramiyakodani, Kyotanabe, Kyoto 610-0321, Japan

^d Logistics Innovation Division, Toshiba Logistics Corporation, 1-14 Nisshin-cho, Kawasaki-ku, Kawasaki 210-0024, Japan

ARTICLE INFO

Article history:

Received 15 April 2013

Received in revised form 14 June 2013

Accepted 3 July 2013

Available online 11 July 2013

Keywords:

Near-field acoustic levitation

Non-contact transporter

Flexural vibration

Finite-element analysis

ABSTRACT

We developed a plate-shaped non-contact transporter based on ultrasonic vibration, exploiting a phenomenon that a plate can be statically levitated at the place where its gravity and the acoustic radiation force are balanced. In the experiment, four piezoelectric zirconate titanate elements were attached to aluminum plates, on which lattice flexural vibration was excited at 22.3 kHz. The vibrating plates were connected to a loading plate via flexible posts that can minimize the influence of the flexure induced by heavy loads. The distribution of the vibration displacement on the plate was predicted through finite-element analysis to find the appropriate positions of the posts. The maximum levitation height of this transporter was 256 μm with no load. When two vibrating plates were connected to a loading plate, the maximum transportable load was 4.0 kgf.

© 2013 Elsevier B.V. All rights reserved.

1. Introduction

In logistics industry and transport systems in factories, objects are often manually transported using pallets, where considerable thrust is needed for heavy load due to the friction force between the pallets and the floor. To reduce the friction, non-contact transport systems based on air bearing have been developed [1], but they required large air compressors and air tubes with sufficient amount of clean air. One of the promising candidates to solve this problem is the technique based on near-field acoustic levitation (NFAL). With this effect, a planner object can be levitated above a vibrating plate via a small air gap due to the acoustic radiation force generated by the ultrasonic field in the gap. There have been many reports to apply the NFAL to transporting silicone waters on large glass plates of liquid crystal display [2–6]. Here, we discuss a non-contact pallet table, where vibrating plates are levitated on a flat floor with acoustic radiation force.

We have so far reported two types of NFAL-based non-contact stages: a sliding table with two triangular cross-sectional guide rails [7] and a self-running bidirectional slider with an aluminum rectangular frame [8]. These stages exploit the traveling waves propagating along the stator guide rails or the slider itself, which induces acoustic streaming along the air gap, and a thrust force is generated to the slider through the viscosity force of air [9,10]. Traveling waves can be generated by two vibrating elements with

a two-phase drive as well [7,8]; one of the vibration elements acts as a generator of sound waves, and the other as an absorber. We have also investigated an ultrasonically levitated slider for a self-running sliding stage for linear movement [11] as well as a non-contact moving two-dimensional stage [12] without guide rails required in the conventional ultrasonically levitated tables [7,8]. However, these rail-free transporters are applicable only to light objects.

In this paper, an NFAL-based plate-shaped non-contact transporter for relatively heavy loads is demonstrated. Four piezoelectric zirconate titanate (PZT) elements were attached to an aluminum plate, on which lattice flexural vibration was excited at 22.3 kHz. Two or four vibration plates were bearing an object with a loading plate, as illustrated in Fig. 1. To minimize the influence of the deflection induced by heavy loads, the vibrating plates were connected to the loading plate via flexible supporting posts. With no load, the maximum levitation height of this transporter was 256 μm . When two vibrating plates were connected to a loading plate, the maximum transportable load of 4.0 kgf was achieved.

2. Configuration of vibrating plate

The configuration of the self-levitation vibrating plate is shown in Fig. 2a–c. The vibrating plate consisted of a square aluminum plate ($2 \times 78 \times 78 \text{ mm}^3$) and four PZT elements ($1 \times 18 \times 18 \text{ mm}^3$; C-203, Fuji Ceramics). The PZT elements, bonded to the aluminum plate using epoxy, were polarized in the thickness direction. The

* Corresponding author. Tel.: +81 459245052.

E-mail address: ishii@sonic.pi.titech.ac.jp (T. Ishii).

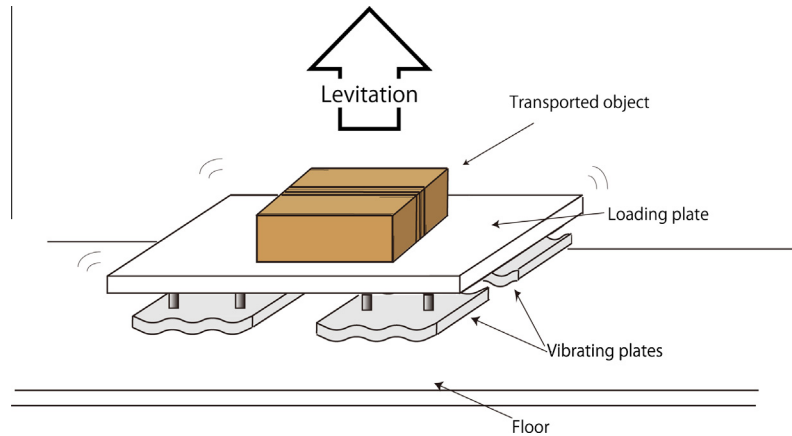


Fig. 1. Concept of self-levitating plate.

mass of the vibrating plate was as light as 42.2 g (68.0 N/m^2). By applying an alternating voltage to the PZT elements, lattice-mode flexural vibration at 22.3 kHz was generated in the aluminum plate, which induced the acoustic radiation force downward to the flat floor.

The dimensions of the aluminum plate and the PZT elements, the locations of the four PZT elements on the aluminum plate, and the flexural vibrating mode were determined with FEA simulation (ANSYS 11.0) [13] so that the vibration displacement amplitude of the vibrating plate was maximized to obtain large levitation force. Fig. 3 shows the simulated optimal distribution of the vibration displacement amplitude, where four nodal lines were observed in both X and Y directions at the resonance frequency of 23.2 kHz. Suitable positions of the PZT elements to maximize the average vibration amplitude over the entire vibrating plate were in every half wavelength of the lattice flexural vibration. The optimal size of the PZT elements (18 mm) was equal to the half wavelength of the flexural vibration.

3. Characterization of the flexural vibrations

The displacement amplitude distribution of the lattice-mode flexural vibration on the prototype was measured using a laser Doppler vibrometer (LDV), as shown in Fig. 4. The vibration mode expected through the FEA (Fig. 3) was successfully excited in the prototype vibrator at 22.3 kHz. All the PZT elements were excited in phase. The flexible posts for connecting the vibrating plate to the loading plate should be fixed at the nodal position of the plate because (1) the flexural vibration on the vibrating plate should not be suppressed and (2) the vibration should not be conveyed to the loading plate. Thus, the positions of the four posts were set, as shown in Fig. 4, to the four points (indicated as “P”) on the nodal lines.

Fig. 5 shows the dependence of the total driving current to the four PZTs on the normal vibration velocity at the edge of the vibrating plate. The force coefficient, i.e. the slope of the dependence, was $\sim 0.59 \text{ N/V}$. Using this value, the vibrating velocity can be estimated simply by measuring the current.

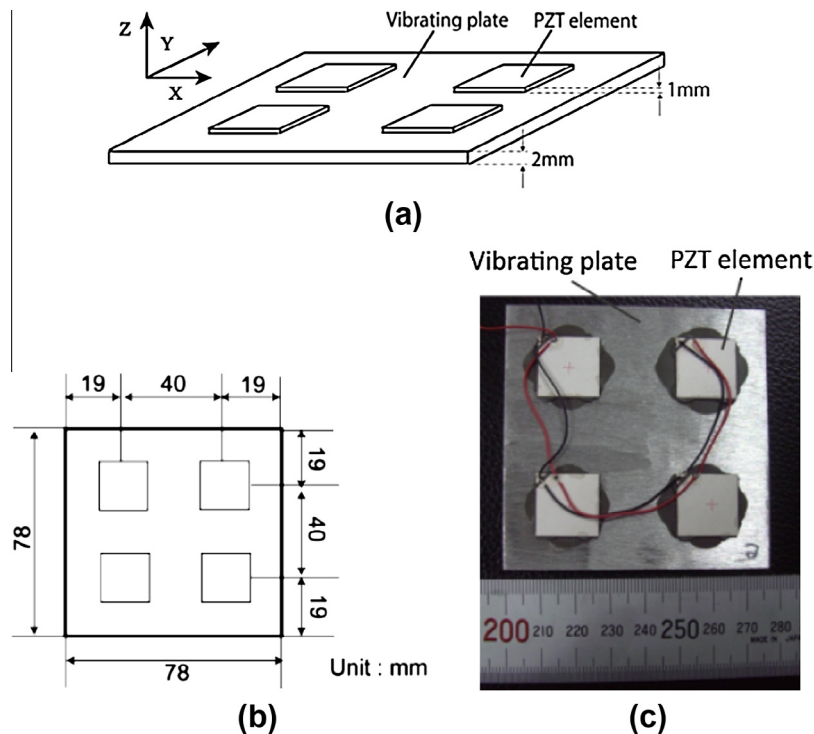


Fig. 2. (a) Configuration, (b) location of the PZTs, and (c) photograph of the vibrating plate.

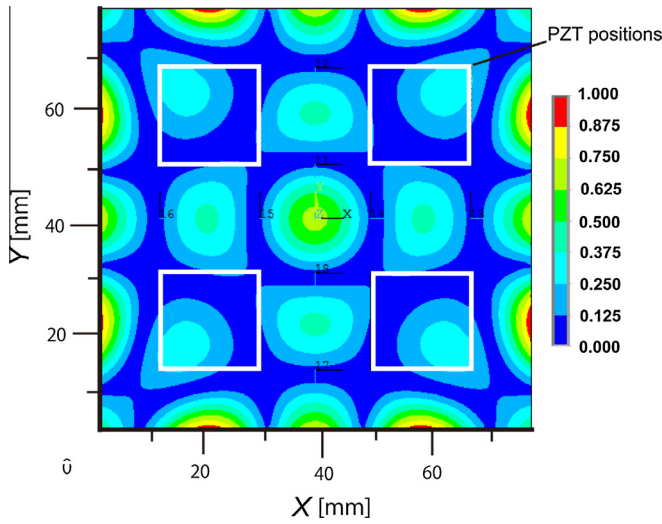


Fig. 3. Simulated distribution of the vibration displacement amplitude on the plate at 23.2 kHz. The vibration amplitude is normalized by its maximum value.

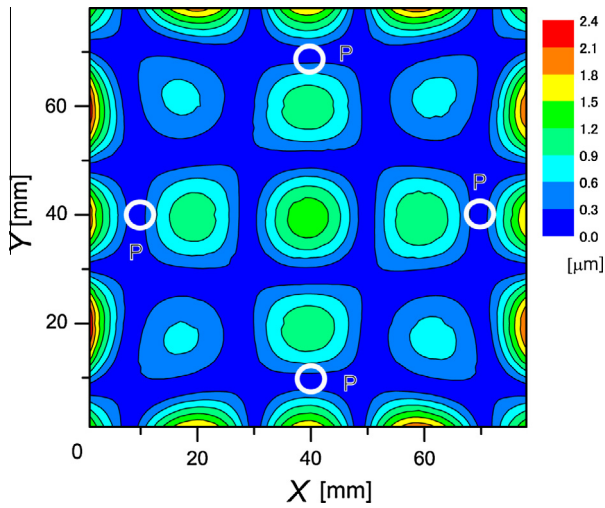


Fig. 4. Measured distribution of the vibration displacement amplitude at 22.3 kHz.

Fig. 6 shows the measured admittance loops of the vibrating plate with and without the posts, from which the resonance characteristics were calculated as described in Table 1. While the resonance frequency and the damped capacitance were almost unchanged, the quality factor and the motional admittance that affect the vibration performance were moderately reduced by connecting the posts. The reduction is within the range applicable to practical use.

4. Levitation characterization

We investigated the levitation characteristics of the vibrating plate. According to the NFAL theories [14,15], when the vibrating mode of a sound source is an in-phase piston vibration mode, the levitation distance of the flat object h is expressed as

$$h = cu\sqrt{\frac{1+\gamma}{4w}}\rho, \quad (1)$$

where c is the sound speed in air, u is the displacement amplitude of the vibration plate, w is the weight of the levitated object, γ is the specific heat ratio in air, and ρ is the density of air. Eq. (1) indicates

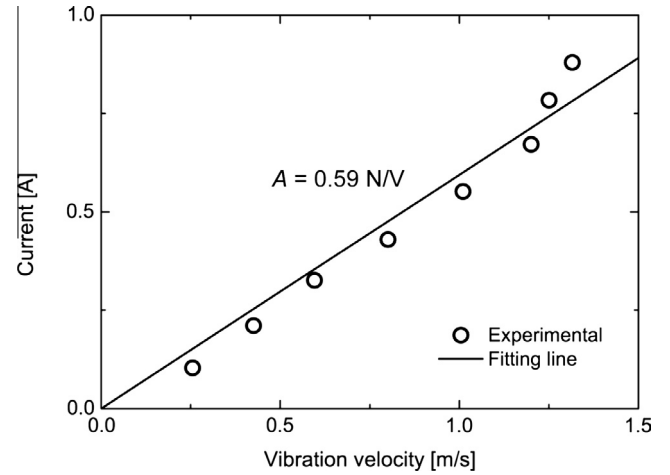


Fig. 5. Total current vs. vibration velocity.

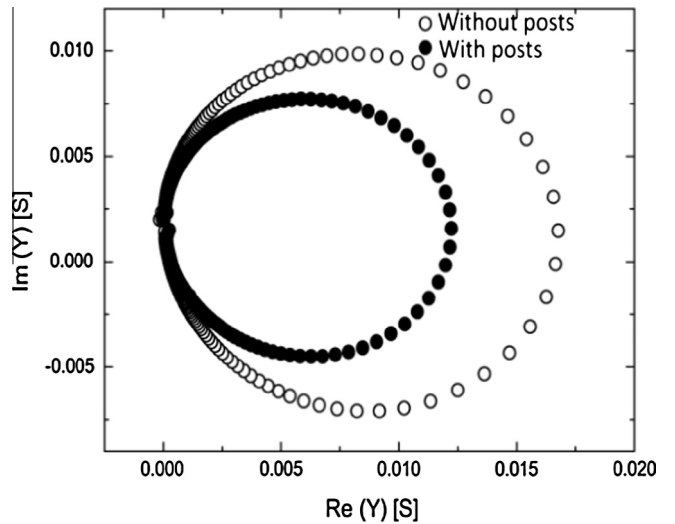


Fig. 6. Admittance loop of the vibrating plate with and without the posts.

Table 1

Resonance characteristics of the vibrating plate.

	Without posts	With posts
Resonance frequency f_0 (kHz)	22.28	22.32
Quality factor	811.0	578.8
Motional admittance Y_{m0} (mS)	16.76	12.39
Damped capacitance C_d (nF)	15.29	15.72

that the levitation distance h is proportional to u and $w^{-0.5}$. Fig. 7 shows the levitation distance measured at the edge of the vibrating plate as a function of the maximum displacement amplitude of the vibrating plate. The levitation distance was measured with a digital microscope (VH-8000 and VH-Z450, Keyence, Co.). In the range of u from 7 to 12 μm , h was proportional to $u^{0.5}$, though h should be in theory proportional to u . When the vibration displacement amplitude was 26.0 μm , the maximum levitation distance of 256 μm was obtained. The experimental values of h were approximately 30% of the theoretical values, probably because the sound field leakage between the vibrating plate and the substrate is not taken into consideration in deriving Eq. (1) and because part of the sound waves transmitted from the 2-mm-thick vibrating plate was attenuated and converted to heat in the air gap between the plate and the bottom substrate. In addition, the difference is attributed to

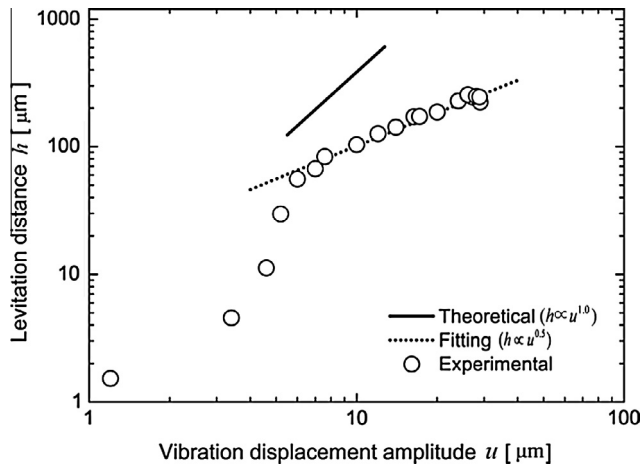


Fig. 7. Measured levitation distance of the vibrating plate as a function of the vibration displacement amplitude.

the assumption in the theoretical model that the vibration mode of the plate is an in-phase piston mode, not a flexural mode. The abrupt reduction in h was observed when u was lower than $7 \mu\text{m}$, which might be caused by energy leakage, as theoretically predicted in Ref. [16].

Next, we connected two vibrating plates to one loading plate using eight posts, as shown in Fig. 8a, and its levitation distance was measured as a function of the weight on the loading plate. Hereafter, the vibrating plate connected with four posts is referred to as a "unit". Cylindrical rods with the diameter of 10 mm and the length of 20–30 mm were employed as the posts. The elastic compliance was performed at both sides of the posts to suppress the vibration transmission to the loading plate by attaching an elastic material, such as a coiled spring (Young's modulus: 206 GPa), silicone rubber (14.2 MPa), urethane (600 MPa), and silicone gel (0.1 MPa), the photographs of which are shown in Fig. 8b. An acrylic plate ($3 \times 80 \times 80 \text{ mm}^3$) was used as a loading plate. Since the quality factor of the vibrating plate with the gel was larger than that with the other three, the levitation distance h was measured as a function of load using one and two units with the gel-attached posts, as shown in Fig. 9. As the levitation distance is reduced by the load, the radiation impedance of the vibrating plate is raised, which indicates that the vibration amplitude changes with the load even if the voltages are the same. In Fig. 9, the voltages applied to the vibrating plate were adjusted so that the vibration displace-

ment amplitude was fixed at $6.0 \mu\text{m}$. The theoretical lines based on Eq. (1) were also provided. As the weight of the loading plate was increased, the levitation distance h was reduced. When the load was under 1 kgf, h with one unit was larger than that with two units. In the case of the load over 2 kgf, levitation was not observed with one unit, whereas clear levitation was observed with two units. The loadable maximum weight of 4.0 kgf was obtained with two units. From these results, the large levitation force appears to be achieved by increasing the number of units.

5. Relationship between pull force and displacement amplitude

Even when the levitating transporter is not completely non-contact, the reduction in the pull force due to the suppression of the friction is practically useful in transporting objects. The pull force in the horizontal direction was measured with a digital force gauge as a function of the mass on the loading plate with one and two units. The relationship between the vibration amplitude and the pull force is summarized in Fig. 10, where the posts with the four materials (described in the previous section) attached were used. The weight of the mass was fixed at 2.0 kgf. Under all the conditions, the pull force was decreased with the increase in the displacement amplitude: for example, the pull force was 1.1 N when the vibration amplitude was $8.0 \mu\text{m}$ with two units and the posts with the gel. This result implies that the pull force was reduced to 75% when compared to that without vibration excitation. With one unit, the pull force was reduced to 45%.

The static deflection at the center of the loading plate caused by the weight of the transported object affects the levitation characteristics. Fig. 11 shows the changes in the pull force when the distances between the two units d were 40 and 80 mm. When a weight of 3 kgf was put on the loading plate, the static deflections were 0.9 and 3.5 mm for $d = 40$ and 80 mm, respectively. While the pull force was reduced by increasing the vibration amplitude, only a slight difference was observed between the results for $d = 40$ and 80 mm. The larger static deflection of the loading plate induces the acoustic streaming from the center to the edges of the vibrating plate, because the sound pressure amplitude at the center part of the vibrating plate is higher than that at the edges. This indicates that part of the acoustic energy in the air layer between the plate and the substrate are transformed to the acoustic streaming and dissipated. In addition, the larger static deflection also means a larger gap between the vibrating plate and the floor, where the sound field is weakened. Therefore, the small static deflection improves the levitation force, leading to the reduction in the pull force.

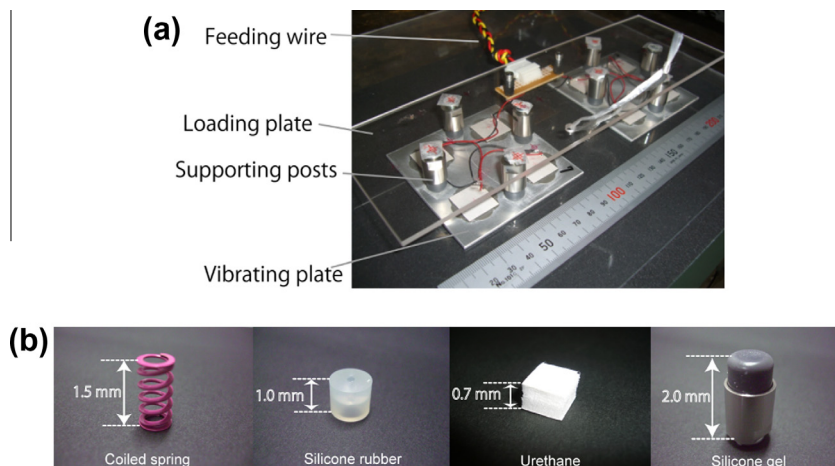


Fig. 8. Photographs of (a) self-levitating plate involving two vibrating plates (i.e., two units), and (b) four kinds of posts used in the experiments.

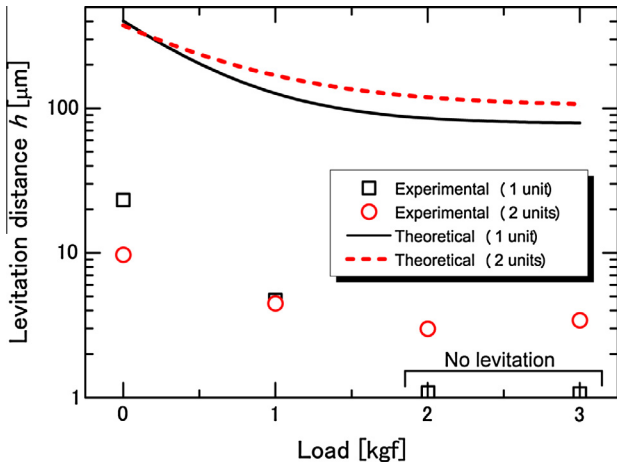


Fig. 9. Levitation distance of the vibrating plate vs. load when gel-attached posts were employed.

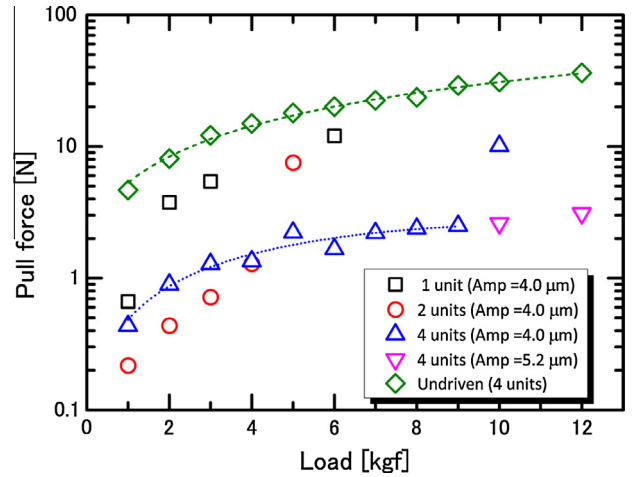


Fig. 12. Measured pull forces as functions of load when the unit number was 1, 2, and 4.

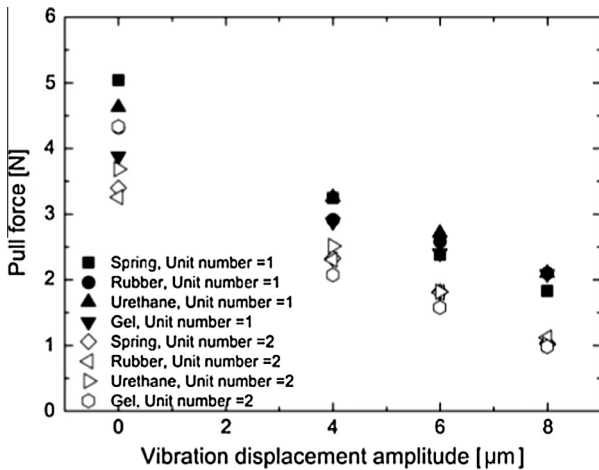


Fig. 10. Relationship between the pull force and the vibration displacement amplitude when the number of unit was 1 and 2.

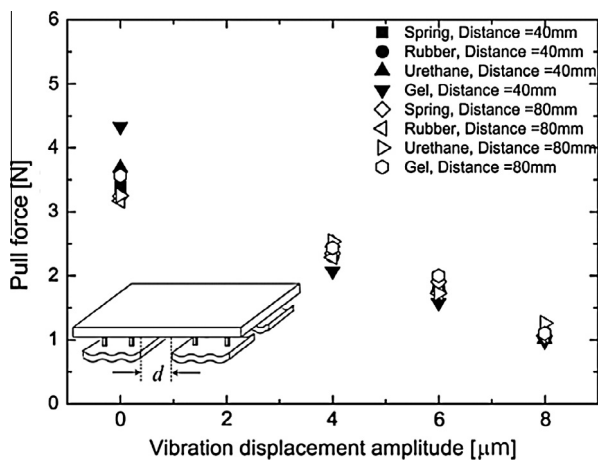


Fig. 11. Relationship between the pull force and the vibration displacement amplitude when the distance between the two units was 40 and 80 mm.

6. Levitation characteristic with four units

Finally, the minimum pull force required to move the units was measured while maintaining the constant vibration amplitude of 4.0 μm and increasing the weight on the loading plate, as shown

in Fig. 12. The number of the units was changed from one to four. With one and two units, the maximum transportable weights were 1 and 4 kgf, respectively. The pull forces were drastically increased to the values without excitation, if the weights over these maximum values were applied. The weight of 9 kgf was transported with four units and the pull force was 2.5 N, which is 1.25 times larger than that with no loading. From comparison between the results with the four units and without excitation, the pull force was decreased to 1/10 by the ultrasound levitation, since the frictional resistance between the vibrating plate and the bottom substrate was reduced. When the vibration amplitude was increased to 5.2 μm , the maximum transportable weight was increased to 12 kgf, while the pull force was not changed under 9 kgf. The electrical power consumption per unit was approximately 13 W.

7. Conclusions

A plate-shaped non-contact transporter exploiting NFAL was developed. The transporter consisted of flexural vibrating plates and a loading plate connected via supporting posts. The acoustic radiation force from the vibrating plates produced the levitation force of the transporter. The configuration of the vibrating plate was determined by use of FEA. The loadable maximum weight of 4 kgf was achieved. The levitation force was increased with the number of units, which decreased the pull force in the horizontal direction. From the results obtained in this study, a 320-kgf load is expected to be carried using about 140 units, with the total input electrical power of 1.8 kW. We believe that the non-contact self-levitating plate presented in this paper will be of great use in transporting heavy objects in logistics with its various advantages including structure simplicity, cost efficiency, and applicability to non-electric/magnetic materials.

References

- [1] G. Obinata, S. Mori, T. Hoshino, K. Ouchi, Air-bearing linear actuator for highly precise tracking, *IEEE Trans. Magn.* 39 (2003) 812–818.
- [2] Y. Hashimoto, Y. Koike, S. Ueha, Transporting objects without contact using flexural traveling waves, *J. Acoust. Soc. Am.* 103 (1998) 3230–3233.
- [3] S. Ueha, Y. Hashimoto, Y. Koike, Non-contact transportation using near-field acoustic levitation, *Ultrasonics* 38 (2000) 26–32.
- [4] T. Amano, Y. Koike, K. Nakamura, S. Ueha, Y. Hashimoto, A multi-transducer near field acoustic levitation system for noncontact transportation of large-sized planar objects, *Jpn. J. Appl. Phys.* 39 (2000) 2982–2985.
- [5] A. Minikes, I. Bucher, Levitation force induced by pressure radiation in gas squeeze films, *J. Acoust. Soc. Am.* 116 (2004) 217–226.
- [6] R. Yano, M. Aoyagi, H. Tamura, T. Takano, Novel transfer method using near-field acoustic levitation and its application, *Jpn. J. Appl. Phys.* 50 (2011). 07HE29-1-07 HE29-5.

- [7] D. Koyama, T. Ide, J.R. Friend, K. Nakamura, S. Ueha, An ultrasonically levitated noncontact stage using traveling vibrations on precision ceramic guide rails, *IEEE Trans. Ultrason. Ferroelect. Freq. Contr.* 54 (2007) 597–604.
- [8] D. Koyama, K. Nakamura, S. Ueha, A stator for a self-running ultrasonically levitated sliding stage, *IEEE Trans. Ultrason. Ferroelect. Freq. Contr.* 54 (2007) 2337–2343.
- [9] T. Yamazaki, J. Hu, K. Nakamura, S. Ueha, Trial construction of a noncontact ultrasonic motor with an ultrasonically levitated rotor, *Jpn. J. Appl. Phys.* 35 (1996) 3286–3288.
- [10] Y. Yamayoshi, S. Hirose, Improvement of characteristics of noncontact ultrasonic motor using acoustically coupled two air gaps, *Jpn. J. Appl. Phys.* 50 (2011). 07HE28-1-07HE28-6.
- [11] D. Koyama, H. Takei, K. Nakamura, S. Ueha, A self-running standing wave-type bidirectional slider for the ultrasonically levitated thin linear stage, *IEEE Trans. Ultrason. Ferroelect. Freq. Contr.* 55 (2008) 1823–1830.
- [12] D. Koyama, K. Nakamura, Noncontact self-running ultrasonically levitated two-dimensional stage using flexural standing waves, *Jpn. J. Appl. Phys.* 48 (2009). 07GM07-07GM07-5.
- [13] Y. Koike, Y. Hashimoto, S. Ueha, Theoretical analysis of acoustic levitation using flexural vibrating plate, Technical report of IEICE, US94-48, 1994, pp. 9–16 (in Japanese).
- [14] B. Chu, E. Apfel, Acoustic radiation pressure produced by a beam of sound, *J. Acoust. Soc. Am.* 72 (1982) 1673–1687.
- [15] C. Lee, T. Wang, Acoustic radiation pressure, *J. Acoust. Soc. Am.* 94 (1993) 1099–1109.
- [16] H. Nomura, T. Kamakura, Theoretical and experimental examination of near-field acoustic levitation, *J. Acoust. Soc. Am.* 111 (2002) 1578–1583.